

# UCLA

## UCLA Previously Published Works

### Title

Processing and properties of SiC/vinyl ester nanocomposites

### Permalink

<https://escholarship.org/uc/item/9rk6167f>

### Journal

Nanotechnology, 15(9)

### ISSN

0957-4484

### Authors

Yong, V  
Hahn, H T

### Publication Date

2004-09-01

Peer reviewed

# Processing and properties of SiC/vinyl ester nanocomposites

Virginia Yong<sup>1</sup> and H Thomas Hahn<sup>1,2,3</sup>

<sup>1</sup> Materials Science and Engineering Department, University of California, Los Angeles, CA 90095, USA

<sup>2</sup> Mechanical and Aerospace Engineering Department, University of California, Los Angeles, CA 90095, USA

E-mail: hyong@ucla.edu and hahn@seas.ucla.edu

Received 6 March 2004

Published 13 August 2004

Online at [stacks.iop.org/Nano/15/1338](http://stacks.iop.org/Nano/15/1338)

doi:10.1088/0957-4484/15/9/038

## Abstract

The feasibility of improving polymer composites was investigated using 30 nm SiC nanoparticles in a vinyl ester resin. Even when the particle loading was less than 4% by weight, the viscosity of the nanoparticle suspension was found to increase much higher than that of microparticle suspension. This phenomenon may be the result of association between nanoparticles and polymer molecules, effectively making the nanoparticles larger. The resulting reduction in the mobility of polymer molecules also led to delayed curing. Ultrasonic mixing did not fully disperse the particles. As a result, the composite strength did not improve although the modulus increased. The use of a dispersant, methacryloxy propyl trimethoxy silane (MPS), improved the dispersion quality and hence the composite strength. The paper discusses the issues involved with processing, characterization and properties of SiC/vinyl ester nanocomposites. Methods of improving the nanocomposite quality are proposed in the paper as well.

(Some figures in this article are in colour only in the electronic version)

## 1. Introduction

Polymer nanocomposites are hybrid structures where one phase has at least one dimension in the nanosize range (usually defined as 1–100 nm). Compared to particles with sizes in the micrometre range, nanoparticles have a large surface area, and consequently, a nanocomposite may exhibit special properties arising from phase interactions at interfaces [1]. Unfortunately, in the nanosize range, dispersion becomes especially critical and difficult because of the large surface-to-volume ratio.

Covalent ceramic materials like silicon carbide (SiC) have been recognized as potential candidates for structural applications because of their superior mechanical properties (strength, stiffness and hardness), chemical (oxidation and corrosion resistance) and thermal stability at high temperatures. The low viscosity coupled with rapid curing rate at room temperature and relatively low cost of vinyl ester resins have led to their extensive use as matrix materials

for reinforced composites. This paper investigates the feasibility of improving polymer composites using 30 nm SiC nanoparticles in a vinyl ester resin.

## 2. Experiment

### 2.1. Materials

The matrix resin used was Derakane momentum 411-350, which is an epoxy vinyl ester resin. The hybrid molecular structure of epoxies and polyesters contributes to its excellent mechanical strength, as well as chemical and solvent resistance. The aromatic rings provide good mechanical properties and heat resistance. The ether linkage contributes to good chemical resistance. The ester groups and two C=C double bond linkages are located at the end of the polymer chains, which lead to the high reactivity of the terminal unsaturation of vinyl ester resin. Curing was achieved by addition of 2.0 wt% of Trigonox 239A catalyst. 0.3 wt% of

<sup>3</sup> Author to whom any correspondence should be addressed.

cobalt naphthenate (CoNap) promoter was added to promote the decomposition of the catalyst during room temperature cure. 30 nm SiC powder with composition of SiC more than 95%, oxygen 1–1.5% and carbon 1–2% was used. The  $\beta$ -SiC, a cubic zinc blende structure or 3C-SiC with a stacking order A, B and C (where A, B and C denote the three distinct layers), is the majority phase as specified by the manufacturer.

A nonionic methacrylate ester-functional silane, *gamma*-methacryloxy propyl trimethoxy silane (MPS), was chosen as the coupling agent and dispersant. The coupling mechanism depends on a stable link between the organofunctional group (Y, chosen for chemical reactivity with the vinyl ester resin) and hydrolysable groups (X, intermediates in formation of silanol groups for bonding to SiC surfaces) in compounds of the structure  $X_3SiRY$ . Best wet-strength retention is obtained with three hydrolysable groups on silicon. Although there are three reactive silanols ( $\sim Si-OH$ ) per molecule, reactive sites on a SiC particle surface are so spaced that not more than one silanol group per MPS molecule can bond to the SiC surface. The remaining silanol groups may condense with adjacent silanols to form a siloxane layer (Si-O-Si) or remain partly uncondensed at the surface. The organofunctional group 'methacrylates' exhibits the best wet strength with polyester and the functional group  $-(CH_2)_3Si(OMe)_3$  of methacrylate additive exhibits the highest flexural strength of polyester glass laminates [2]. The functional group  $-(CH_2)_3Si(OMe)_3$  reacts with hydroxylated SiC surfaces through hydrogen bonding and through covalent siloxane (Si-O-Si) bonds [3]. In addition, the organofunctional group 'methacrylates' could copolymerize with styrene monomers in the vinyl ester during cure [4]. Therefore, MPS may act as a bridge to bond the SiC to the vinyl ester resin with a chain of covalent bonds. This could lead to the strongest interfacial bond.

## 2.2. Characterization of SiC nanoparticles

Transmission electron microscopy (TEM) was used to characterize the size distribution of SiC nanoparticles. TEM sample preparation was carried out by diluting the SiC nanoparticles with isopropyl alcohol (IPA) and sonicating the suspension at 40 W for 10 min. A drop of the sonicated suspension was then put on the Prod #01800 Ted Pella 200 mesh specimen support film grids. Only SiC nanoparticles were left for TEM examination on the support film after the evaporation of IPA solution.

As-received SiC nanoparticles were heated both in air and in nitrogen to 1000 °C using a thermogravimetric analysis (TGA) to examine the moisture adsorption on the SiC surface. Weight changes of the specimen were recorded at 10 °C min<sup>-1</sup>.

## 2.3. Processing and characterization of SiC/vinyl ester nanocomposites

The MPS functions as a finish or surface modifier and may theoretically be only a monomolecular layer, but in practice it may be several monolayers thick. The calculation of the amount of MPS dosage was as follows:

$$m_f = \frac{M_f m_s A_{sp}}{A_f} + M_f CMC_f V_l$$

with  $m_s$  = mass of SiC nanoparticles = 1 wt% of 15 ml of vinyl ester = 0.156/1000 kg;  $A_{sp}$  = specific surface area of SiC (diameter of 1  $\mu m$ ) = 1875 m<sup>2</sup> kg<sup>-1</sup>;  $M_f$  = molar mass of MPS = 248.4/1000 kg mol<sup>-1</sup>;  $A_f$  = molar area coverage of MPS = 10<sup>5</sup> m<sup>2</sup> mol<sup>-1</sup>. This corresponds to 6 molecules adsorbed per nm<sup>2</sup> (or 100 Å<sup>2</sup>) of surface.  $V_l$  = volume of liquid (m<sup>3</sup>);  $CMC_f$  = saturated solubility of MPS in resin = assume 0 mol m<sup>-3</sup>.

Therefore, the monolayer dose  $m_f$  for 1  $\mu m$  SiC is  $7.266 \times 10^{-4}$ /1000 kg, which is equal to 0.466 wt% of SiC. This monolayer dosage calculation is in agreement with the general guidelines of 1–3 wt% of SiC for particles in the 0.1–3  $\mu m$  size range. The general guideline corresponds to  $\sim 4$  monolayers. For SiC with an average diameter of 30 nm, specific surface area  $A_{sp}$  is 62 500 m<sup>2</sup> kg<sup>-1</sup>. Thus, the monolayer dose  $m_f$  for 30 nm SiC is 0.0242/1000 kg. For 4 monolayers, the MPS dosage is 0.104 g. It is equivalent to 67 wt% of SiC.

Since the energy of wetting must exceed the interparticle binding energy and the process is liquid diffusion limited, mechanical force is required (we used an ultrasonic disperser and magnetic stirrer) to separate the agglomerates of particles and permit the MPS to adsorb onto the unwet portions of the SiC surface. SiC/vinyl ester nanocomposites were mixed under the following conditions:

- Resin (Derakane momentum 411-350) volume: 100 ml.
- Sonication (24 W) + magnetic stirring (cooled with compressed air): 1 h.
- Degassing in vacuum for 1 h.
- TrigonoX (catalyst): 2.0 wt%.
- CoNap (promoter): 0.3 wt%.
- Post-cure at 85 °C for 1 h.

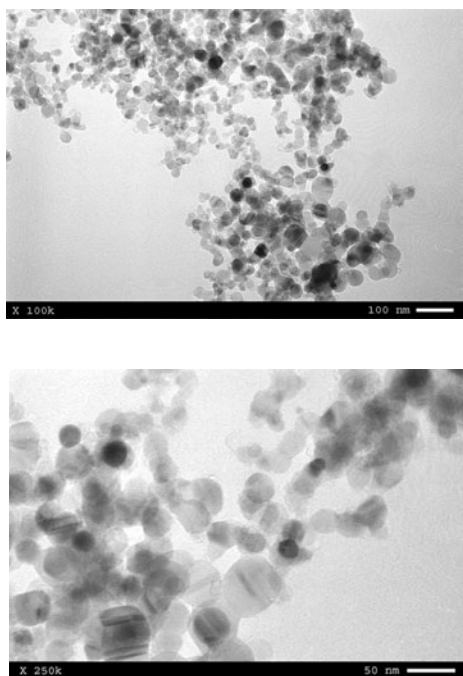
Nanoparticle dispersion was characterized by both optical microscopy and AFM in force modulation (contact mode) and in phase imaging (tapping mode). The different stiffnesses of the SiC and vinyl ester resin matrix are manifested by the two different signals with a phase difference, and SiC particles (stiffer component) were seen as locations with brighter contrast. The multi-component compositional imaging using AFM is in full agreement with TEM [5–7].

## 3. Results and discussion

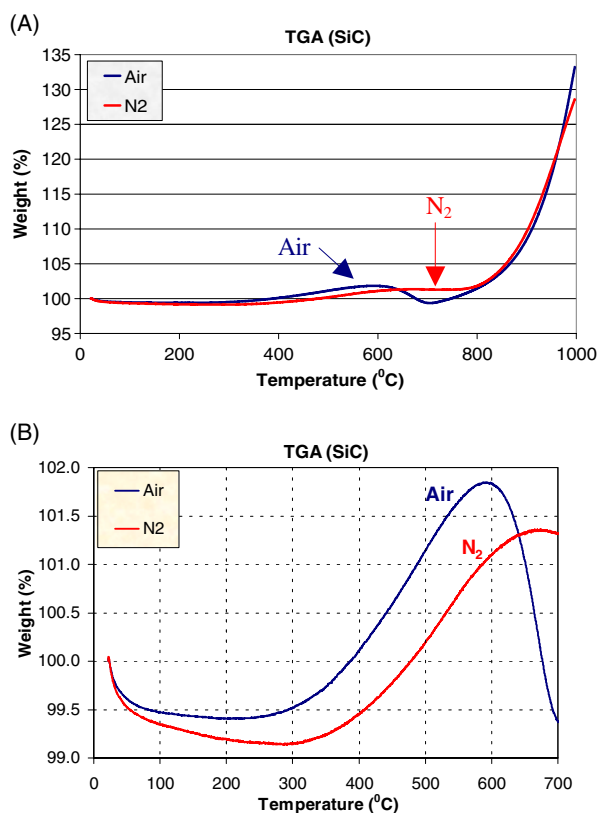
### 3.1. Characterization and pre-treatment of SiC nanoparticles

Figure 1 shows TEM micrographs at 100k $\times$  and 250k $\times$ , which indicate a good size distribution of SiC nanoparticles with an average diameter of around 30 nm, as specified by the manufacturer.

TGA at a heating rate of 10 °C min<sup>-1</sup> shows a maximum weight loss at 200 °C as shown in figure 2, which was assigned to the loss of water. This water derived partially from endothermic condensation of Si-OH groups and partially from evaporation of free water which was adsorbed due to the hydrophilic SiC surface [2, 8]. Water increases one particle surface's affinity for another, which excludes organic molecules within agglomerates. Also, water is difficult to remove from particle surfaces once these are immersed in organic liquids, as illustrated by the considerably higher heat of



**Figure 1.** TEM micrographs of SiC nanoparticles at 100k $\times$  and 250k $\times$ .



**Figure 2.** TGA shows a maximum weight loss at 200 °C. (A) TGA of as-received SiC nanoparticles. (B) Enlarged view at a temperature range from 0 to 700 °C.

wetting by water compared to organic liquids [9]. Therefore all SiC nanoparticles were pre-treated by vacuum baking at 200 °C for 24 h to remove the adsorbed moisture. A minor oxidation started at approximately 260 °C followed by the main

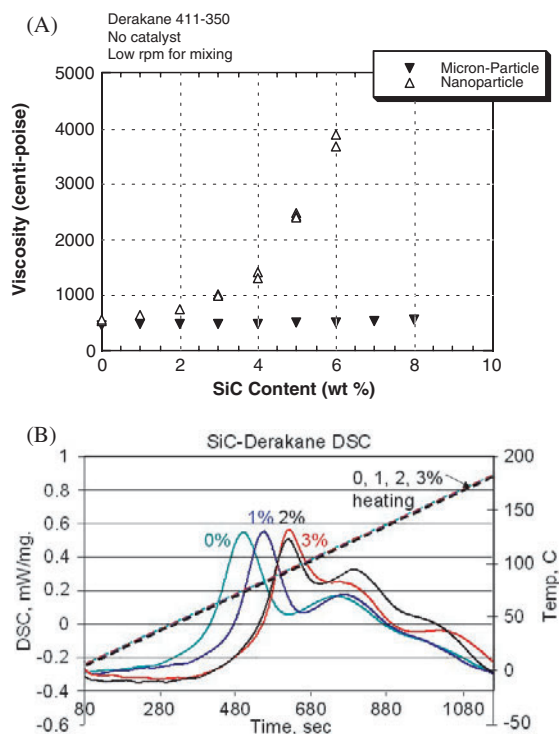


**Figure 3.** Rheology and cure kinetics of SiC/vinyl ester nanocomposites. (A) Viscosity versus SiC for micron- and nano-particles (Courtesy of Pennsylvania State University). (B) DSC curves for SiC/vinyl ester system at 10 °C min<sup>-1</sup>.

oxidation process beginning at approximately 750 °C [10], which resulted in the weight increase. The weight loss began at approximately 600 °C in air and is attributed to the oxidation of carbon [11].

### 3.2. Rheology and cure kinetics

The SiC nanoparticles with no surface treatment raise the viscosity of the suspension much more rapidly than the micron-size SiC particles. Also, the viscosity of SiC filled vinyl ester resin reaches a critical level (1500 cP) for resin transfer moulding, at 4 wt% loading of SiC nanoparticles, figure 3(A) [12]. Differential scanning calorimetry (DSC) was performed to study the kinetics of the curing reactions in the SiC filled resin. Figure 3(B) shows the effect of SiC nanoparticles on the cure and indicates that with an increase in the SiC concentration, the exotherm peak (corresponding to the maximum reaction rate) is shifted to higher temperature, suggesting that the SiC nanoparticles retards the reaction. The scanning calorimetry traces appear to be composed of at least two exothermic peaks and so are suggestive of two reaction processes. The first peak is due the copolymerization of the styrene with the vinyl ester vinylene groups, while the second peak (or shoulder) is caused by styrene homopolymerization or grafting reaction of styrene along vinyl ester chains [13].

The viscosity of a suspension increases as either the particle concentration increases or the size of particles decreases [14]. The cure kinetics is dependent on both filler type and content for the system. The SiC nanoparticles, due to their high surface energy coupled with the high surface area, attract the hydrophilic polar portion of vinyl ester molecules

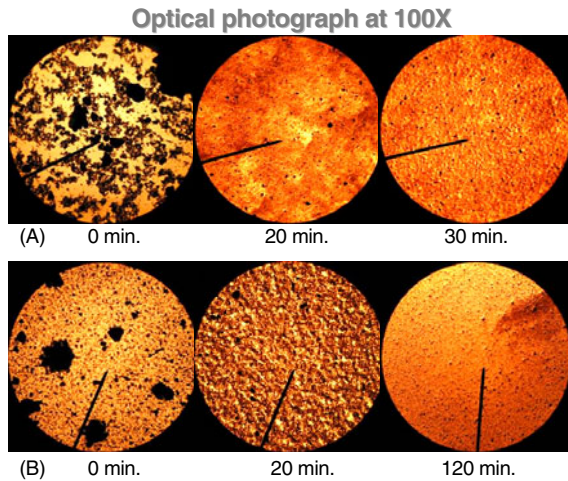


**Figure 4.** Dispersion quality of SiC/vinyl ester samples with different sonication time (A) 1 vol%—20 ml; (B) 1 vol%—120 ml.

resulting in the mobility reduction of polymer molecules. This led to both increased viscosity and delayed curing. An increased amount of catalyst and promoter or a higher cure temperature could be used to shorten the gel time [15].

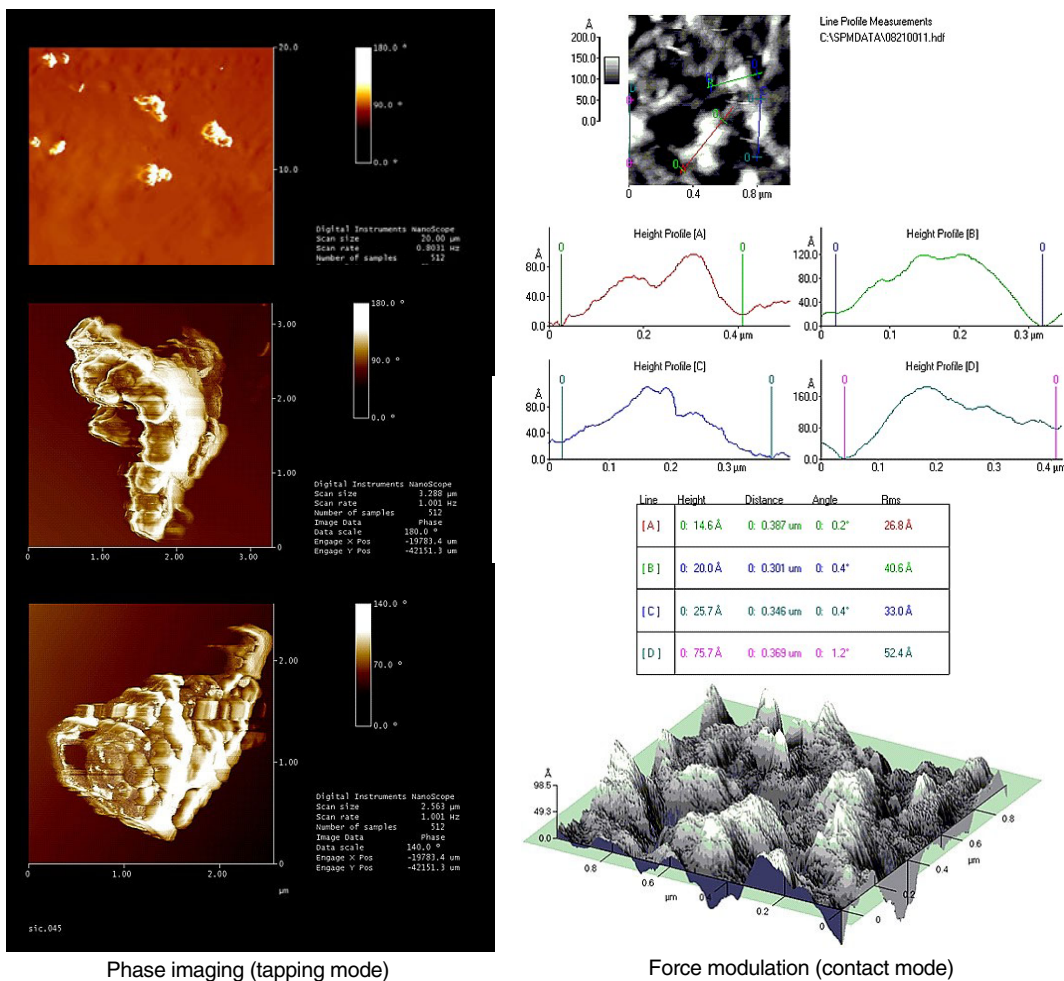
### 3.3. Characterization of SiC/vinyl ester nanocomposites

Optical photographs of figure 4 show the state of dispersion of untreated-SiC particles in vinyl ester resin after sonication. As the resolution of optical microscopy limited by the wavelength of visible light is around  $0.5 \mu\text{m}$  at a magnification of  $2k\times$ , optical photographs at  $100\times$  confirmed the agglomerated SiC nanoparticles at micron scale. The optical inspection indicates that a homogeneous mixture (to a certain extent) was obtained by sonication, however ultrasonic agitation could not break up all of the agglomerates [16].

Particle dispersion characterization via AFM confirmed the better dispersion with the addition of MPS as compared to without MPS. An average agglomerated particle size of  $0.351$  and  $0.647 \mu\text{m}$  were found for SiC/vinyl ester with and without MPS, respectively. Figure 5 shows the AFM images in phase imaging (tapping mode) and in force modulation (contact mode) for the SiC/vinyl ester specimen with MPS.

### 3.4. Flexural properties and fracture analysis

Three-point bending tests were carried out per ASTM D790 ‘Standard Test Methods for Flexural Properties of Unreinforced and Reinforced Plastics and Electrical Insulating



Phase imaging (tapping mode)

Force modulation (contact mode)

**Figure 5.** AFM for dispersion characterization—SiC/vinyl ester with MPS (67 wt% of SiC).

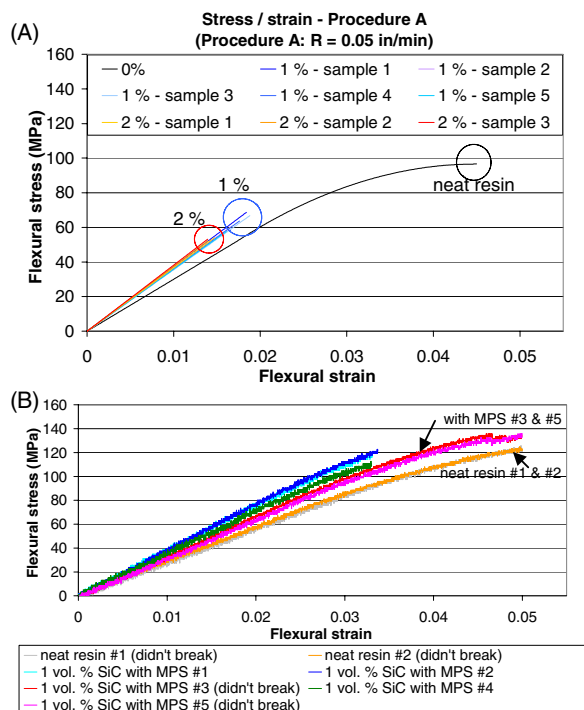


**Figure 6.** Stress versus strain curve of (A) 0, 1, 2 vol% SiC without MPS; (B) 0%, 1 vol% SiC with MPS.

Materials' using procedure A. As Young's modulus of  $\beta$ -SiC (3C) in the  $\langle 100 \rangle$  direction is 392–694 GPa [17] which is a hundred times stiffer than the vinyl ester matrix, the modulus increases when the SiC volume fraction increases, as shown in figure 6 and table 1.

A change in the nature of the interface and dispersion quality at constant volume fraction does not have a significant influence on the modulus, but is essential in determining both the strength and toughness of the composite [18, 19]. Strength increases with the addition of MPS but decreases without MPS. The increase in strength is likely attributable to the better dispersion quality as observed under the optical microscope and AFM (figure 5), lower porosity [2], and a stronger interfacial bonding between the SiC nanoparticles and vinyl ester resin as a result of the MPS addition. For mixing without dispersant, higher particle loading introduces larger and more loosely assembled nanoparticle agglomerates, which act as the stress concentrators causing a decrease in strength.

Fracture analysis was performed on fractured samples from three-point bending tests. The fracture mechanism of neat resin was investigated as a control. The neat resin is characterized by an unstable crack propagation behaviour, which causes failure when the load reaches its critical value. Optical photographs at  $100\times$  of the fracture plane in neat resin show the hackle markings in the direction of crack propagation, shown in figure 7(A), typical of cleavage brittle fracture. The crack was initiated at the sample surface where bending stress is maximum. Optical photographs of fracture planes containing embedded SiC nanoparticles indicate changes in the fracture mechanism from that of neat resin, figures 7(B) and (C). Yielded zone (shear deformation) and crazes (matrix crazing, preceding a propagating crack) were observed at the crack tip [20]. The crack initiation site observed is at the subsurface

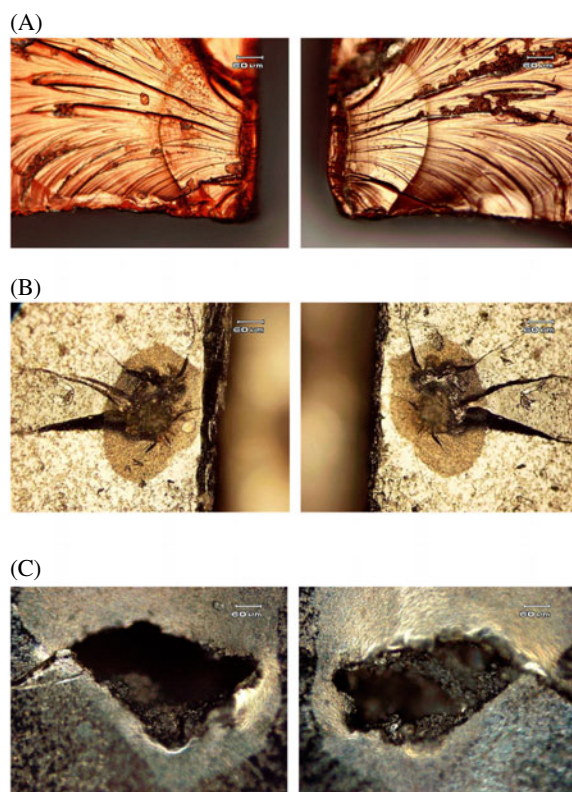


**Figure 7.** Fractography of fracture surfaces. (A) Crack initiation site of a neat resin sample. (B) 1 vol% SiC, bright field image, left and right fracture half at crack initiated site. (C) 1 vol% SiC, dark field image, left and right fracture half at crack initiated site which shows two-interacting inclusions.

**Table 1.** Summary table of the matrix's flexural properties.

SiC (vol%)	Mixing condition	Ultimate flexural stress $\sigma_{max}$ (MPa)		Flexural modulus $E$ (GPa)	
		Mean	SD	Mean	SD
0	Neat resin	116	16	2.9	0.11
1	Without MPS	63	4	3.6	0.07
2		53	1	3.7	0.07
1	With MPS	126	11	3.5	0.28

SiC nanoparticle agglomerated site. The SiC nanoparticles appeared to be debonded from the vinyl ester matrix.

#### 4. Conclusions

Because the SiC nanoparticles are small ( $\sim 30$  nm) and their surface hydrophilic, as well as the high surface energy of SiC acting as the driving force for agglomeration, their dispersion is difficult in a vinyl ester (oleophilic system) resin. Similar behaviour was reported in other material systems [21–23]. The modulus increases by adding SiC nanoparticles regardless of the dispersion quality, whereas strength is highly sensitive to dispersion quality and increases with the addition of MPS but decreases without MPS. Hence a well-dispersed SiC is required to improve the nanocomposite quality. One solution involves a flushing operation. SiC is first dispersed in a long-chain alcohol (six carbons or greater) to which is added a

paraffinic hydrocarbon, octane to dodecane [9, 24]. R–OH are nonionic molecules which rely on hydrogen bonding primarily and van der Waals forces secondarily to attach themselves to SiC particle surfaces and serve as dispersant. Chain length is a factor in dispersion and a separation of 20–60 nm is necessary to overcome the van der Waals forces for colloid stability, but the eight carbon rule (oleophilic–hydrophilic balance point) is generally a workable guide for dispersant design. A well-designed experiment would be able to tell whether the added surfactant would have any adverse side effects on the structural properties of composites.

### Acknowledgments

We would like to thank the Air Force Office of Scientific Research (L Lee) and the US Army Natick Laboratory (J Song and M Sennett) for financial support through AFOSR Grant F49620-02-1-0414, Dr John W Goodman for his advice and to Alessandro Dini for TEM micrographs.

### References

- [1] Roco M C 1999 *J. Nanoparticle Res.* **1** 1
- [2] Plueddemann E P 1991 *Silane Coupling Agents* (New York: Plenum)
- [3] Philipse A P and Vrij A 1989 *J. Colloid Interface Sci.* **128** 121
- [4] Ishida H and Koenig J L 1980 *J. Polym. Sci. B* **18** 1931
- [5] Meyers R A 2000 *Encyclopedia of Analytical Chemistry* (New York: Wiley)
- [6] Potschke P *et al* 2004 *Eur. Polym. J.* **40** 137
- [7] Karger-Kocsis J 2003 *Compos. Sci. Technol.* **63** 2045
- [8] Preiss H *et al* 1995 *Carbon* **33** 1739
- [9] Conley R F 1996 *Practical Dispersion* (New York: Wiley)
- [10] Das D *et al* 2001 *Diamond Relat. Mater.* **10** 1295
- [11] Brewer C M *et al* 1999 *J. Sol–Gel Sci. Technol.* **14** 49
- [12] Lee B L *et al* 2001 Processing of macroscopic fiber composites with dispersion of nanoparticles in resin matrix *221st American Chemical Society Natl Mtg, Symp. on Defense Applications of Nanomaterials (San Diego, California, April 2001)*
- [13] Li L *et al* 1999 *Polym. Eng. Sci.* **39** 646
- [14] Han C D and Lem K W 1983 *J. Appl. Polym. Sci.* **28** 743
- [15] Akatsuka M *et al* 2001 *Polymer* **42** 3003
- [16] Wei D *et al* 2002 *J. Nanoparticle Res.* **4** 21
- [17] Harris G L 1995 *Properties of Silicon Carbide (EMIS Datareviews Series No. 13)* (London: INSPEC, Institution of Electrical Engineers)
- [18] Nielsen L E and Landel R F 1994 *Mechanical Properties of Polymers and Composites* (New York: Dekker)
- [19] Singh R P *et al* 2002 *J. Mater. Sci.* **37** 781
- [20] Smith B W and Grove R A 1986 Failure analysis of continuous fiber reinforced composites and failure analysis of polymers *Metals Handbook* vol 11 (Metals Park, OH: ASM International)
- [21] Ng C B *et al* 1999 *Nanostruct. Mater.* **12** 507
- [22] Evora V M F and Shukla A 2003 *Mater. Sci. Eng. A* **361** 358
- [23] Chow P Y and Gan L M 2004 *J. Nanosci. Nanotechnol.* **4** 197
- [24] Okuyama M *et al* 1989 *J. Am. Ceram. Soc.* **72** 1918